JOURNAL OF GEOPHYSICAL RESEARCH, VOL. 99, NO. A7, PAGES 13,425–13,436, JULY 1, 1994

Concerning flux erosion from the dayside magnetosphere

N. A. Tsyganenko

NASA Goddard Space Flight Center, Greenbelt, Maryland

D. G. Sibeck

Applied Physics Laboratory, Johns Hopkins University, Laurel, Maryland

Abstract. The dayside magnetopause moves inward during periods of southward interplanetary magnetic field in response to decreases in the outer magnetospheric magnetic field strength. We consider possible causes for the magnetic field strength decreases and demonstrate that they are consistent with increases in the region 1 Birkeland and cross-tail currents. We reexamine the well-known series of magnetopause crossings by OGO 5 on March 27, 1968, to demonstrate that they provide evidence for two intervals of gradual inward magnetopause motion associated with magnetic flux erosion and also for two intervals of inward magnetopause motion associated with sharp increases in the solar wind dynamic pressure.

Introduction

When stationary, the dayside magnetopause lies along the locus of points where the component of the solar wind dynamic pressure normal to the nominal magnetopause ($nMV^2\cos^2\theta$), converted into a proportional magnetosheath magnetic and thermal pressure, balances the magnetospheric magnetic pressure ($B^2/2\mu_0$) [e.g., *Spreiter et al.*, 1966]:

$$p = knMV^2\cos^2\theta = B^2/2\mu_0 \qquad (1)$$

Here we neglect the magnetic and thermal pressures in the solar wind upstream of the bow shock under the assumption that they are quite small compared to the solar wind dynamic pressure and therefore make only a negligible contribution to the dayside pressure balance. We also assume that the plasma pressure makes a negligible (<10%) contribution to the total pressure in the outer magnetosphere. The examples of dayside magnetopause crossings presented by *Paschmann et al.* [1986] suggest that the latter assumption is valid, at least during periods of southward interplanetary magnetic field (IMF). Equation (1) indicates that variations in either the solar wind dynamic pressure or the magnetospheric magnetic pressure may upset pressure balance at the magnetopause and therefore cause magnetopause motion. It also allows the component of the solar wind dynamic pressure applied normal to the local magnetopause to be determined from magnetospheric magnetic field strengths observed just inside magnetopause crossings.

The magnetospheric magnetic field $\mathbf{B}$ is the sum of contributions from the Earth's dipole, $\mathbf{B}_d$ ($\alpha\ 1/R^3$), the Chapman–Ferraro or magnetopause currents $\mathbf{B}_{cf}$, the ring current $\mathbf{B}_{rc}$, the magnetotail current $\mathbf{B}_t$, and the Birkeland currents $\mathbf{B}_b$, whose locations were illustrated by *Potemra* [1984]. Assuming symmetry with respect to the planes Y_{gsm} and $Z_{gsm} = 0$, the vector sum of the fields at the subsolar point ($R = R_{ss}$) reduces to the scalar sum of their Z components:

Paper number 94JA00719.
0148-0227/94/94JA-00719$05.00

$$B(R_{ss}) = B_d + B_{cf} + B_{rc} + B_t + B_b \qquad (2)$$

The contribution from the Chapman–Ferraro currents to the magnetic field strength just inside the subsolar magnetopause is proportional to the dipolar term, that is, $B_{cf} = (2f - 1)B_d$ [*Schield* 1969], and the contribution to the subsolar magnetospheric magnetic field from the dipole term is clearly proportional to $1/R_{ss}^3$.

The ring current's contribution to the subsolar magnetic field can be roughly estimated as

$$B_{rc} = M_{RC}/R_{ss}^3 \qquad (3$$

where M_{RC} is the magnetic moment of the ring current. As a crude approximation, magnetospheric expansions and contractions in response to changes of the solar wind dynamic pressure do not change M_{RC} [*Stern*, 1985]. For this reason, we could account for the term B_{rc} in (2) by multiplying B_d by a constant factor $A \sim 1.1$–1.3. Because the ring current magnitude also depends on other factors, we choose to retain the term B_{rc} in the form given by (3).

The last two terms on the right-hand side of (2) are also functions of R_{ss}, but given their relatively large scale sizes, it is reasonable to assume that they remain nearly constant in comparison with the first three terms. Solving (1)–(3) for the equilibrium standoff distance R_{ss}, we obtain

$$R_{ss} = [(2fM_E + M_{RC})]^{1/3}[(2\mu_0 p)^{1/2} - (B_t + B_b)]^{-1/3} . \quad ($$

Equation (4) predicts that the magnetopause moves inward for an increase in p [e.g., *Mead and Beard*, 1964] or a decrease in the contributions from the terms M_{RC}, B_t, and/or B_b [e.g., *Russell et al.*, 1974].

Many statistical studies confirm that the dayside magnetopause moves inward in the manner predicted by (4) when the solar wind dynamic pressure increases [e.g., *Fairfield*, 19 *Holzer and Slavin*, 1978]. Several case and statistical studies provide important evidence indicating that the remaining terms on the right side of (4) are significant. *Aubry et al.* [19 reported a seminal case study that indicates that the dayside magnetopause moves inward during periods of southward IM

Several statistical studies confirm that the dayside magnetopause lies earthward of its mean position during periods of southward IMF [e.g., *Fairfield*, 1971; *Holzer and Slavin*, 1978; *Sibeck et al.*, 1991; *Petrinec et al.*, 1991]. We interpret these studies as indicating that the sum of the latter two terms in (4) diminishes in the outer dayside magnetosphere during periods of southward IMF. Accurate models of all the magnetospheric current systems are clearly essential in order to determine the contribution of each to the subsolar magnetospheric magnetic field strength, and therefore the location where pressure balance can be maintained, as a function of the IMF orientation. The purpose of this paper is to consider each current system in turn, calculate the corresponding magnetic field perturbation just inside the dayside magnetopause, and use pressure balance to estimate the amplitude of the corresponding magnetopause motion. In particular, we will show that perturbations in the outer magnetospheric magnetic field strength and pressure, which are associated with fluctuations in both the region 1 Birkeland and cross-tail currents, suffice to account for the observed inward motion of the magnetopause during periods of southward IMF. We then reexamine the unique case study of *Aubry et al.* [1970], confirm and quantify their results, and extract new information concerning the erosion of the dayside magnetosphere during periods of southward IMF.

The Chapman–Ferraro Current

As originally suggested by *Chapman and Ferraro* [1931], currents on the magnetopause confine the magnetospheric magnetic field to a cavity and enhance magnetic field strengths within that cavity. To separate the northward magnetospheric magnetic fields from those in the magnetosphere, the Chapman–Ferraro currents must increase during periods of southward IMF and decrease during periods of northward IMF. One might conclude, at first glance, that the required increase in dayside currents during periods of southward IMF enhances outer magnetospheric magnetic field strengths. However, the resulting pressure imbalance at the magnetopause would drive the magnetopause outward during periods of southward IMF, and not inward as observed.

The apparent paradox can be resolved by noting that as long as there is no violation of the ideal shielding condition, variations in the magnetopause currents due solely to changes in the IMF orientation do not induce any change in the magnetic field inside the magnetosphere and hence cannot upset the pressure balance. This can be better understood by representing the net Chapman–Ferraro current as a superposition of two separate current systems: one that shields the magnetosphere from external sources and a second that shields the magnetosheath from internal (magnetospheric) sources. The magnetopause current density at any point is thus the sum of two terms: $\mathbf{j}_{cf} = \mathbf{j}_{cf}(e) + \mathbf{j}_{cf}(i)$. Although the former term varies in response to the IMF fluctuations, its integrated contribution to the net field at any point inside the magnetosphere remains zero, provided that shielding is ideal. Should the latter condition be violated for some reason (e.g., the inability of the magnetopause current layer to supply a current sufficient to produce the required magnetic field jump ΔB at the magnetopause), some fraction of the magnetosheath magnetic field will penetrate into the magnetosphere, some of the preexisting magnetopause current will be diverted, and the shape of the magnetopause will change.

We will address changes in the shape of the magnetosphere here and leave consideration of IMF penetration and current diversion until later. Parameter f in (4) describes the contribution of the Chapman–Ferraro currents to the subsolar magnetospheric magnetic field strength as a function of the magnetopause shape (but not its dimensions). Observations indicate that the elliptical magnetopause shape remains nearly constant in response to variations in the solar wind dynamic pressure, but varies somewhat in response to changes in the IMF orientation [*Sibeck et al.*, 1991; *Roelof and Sibeck*, 1993]. Consequently, f is primarily a function of IMF B_z. Parameter f varies from 1 for a planar magnetopause to 1.5 for a spherical magnetopause. Since the shape of the dayside magnetopause remains elliptical over the full range of observed solar wind parameters, f probably remains in close proximity to the value of 1.22 appropriate for an elliptical magnetopause that shields a dipole [*Mead*, 1964].

Penetration of an External Magnetic Field

Because many magnetospheric phenomena depend upon the IMF orientation, one might seek to explain the observed inward motion of the dayside magnetopause during periods of southward IMF as the result of the local or global penetration of some fraction of the IMF into the magnetosphere [e.g., *Kovner*, 1972; *Kovner and Feldstein*, 1973; *Voigt*, 1979, 1986]. Including a corresponding term in (4) would indeed require inward motion of the dayside magnetopause during periods of southward IMF. However, there are some inconsistencies in this approach. Although *Cowley and Hughes* [1983] reported that about 20% of the IMF B_y component appears at the dayside geosynchronous orbit, the dayside magnetospheric magnetic field strength must be depressed by an amount several times greater than the IMF B_z component to account for the observed range of magnetopause crossings [*Sibeck et al.*, 1991]. Furthermore, a penetrating external magnetic field would not cause the magnetotail magnetic flux to increase during periods of southward IMF, as observed. The formal superposition of internal and external magnetic fields is a means of avoiding the more fundamental question, which concerns the mechanism by which the external field enters the magnetosphere. Thus, the very concept of IMF penetration is somewhat misleading: it just introduces one more definition but does not help us understand the physics of the process.

In fact, the effects attributed to a penetrating field are consistent with a redistribution of magnetospheric currents and are therefore implicitly contained in the terms B_{cf}, B_t, and B_h of (4). We believe that the gradual inward motion of the dayside magnetopause observed by *Aubry et al.* [1970] is consistent with the gradual variation of one or more magnetospheric current systems.

Ring Current

Variations in the ring current generally have minor, slowly varying, effects upon the location of the dayside magnetopause. *Schield* [1969] argued that the quiet day ring current contributes 8–10 nT to the equatorial magnetospheric magnetic field strength of 60 nT within the range of positions from 10 to 11.5 R_E from Earth but diminishes the geosynchronous magnetic field by ~25 nT. An enhanced ring current, as might occur during a geomagnetic storm with a decrease in *Dst* to −180 nT, should be accompanied by a further 7–8 nT increase in the outer dayside magnetospheric magnetic field strength and a 0.4 R_E outward motion of the dayside magnetopause [*Schield*, 1969].

The timescales for magnetopause motion associated with ring current variations are quite long. Ground observations during geomagnetic storms indicate that the ring current strength decays gradually over the first 10 hours of a geomagnetic storm and then even more slowly during the following 14 hours [*Chapman and Bartels*, 1940]. As a result, it seems likely that variations in the ring current would produce minor changes in the magnetopause position over periods of many hours. *Freeman* [1964] and *Cahill and Patel* [1967] suggested that the magnetopause lies well outside its average position during the recovery phase of storms, but *Schield* [1969] argued that this effect was due to low solar wind dynamic pressures. *Petrinec and Russell* [1993] demonstrated that the magnetopause position is influenced very little by the intensity of the ring current.

Contribution of the Birkeland Currents

The Birkeland currents make a significant and highly variable contribution to magnetospheric magnetic field strengths in the vicinity of the dayside magnetopause. Region 1 Birkeland currents flow into the ionosphere on the dawnside of the Earth and away from the ionosphere on the duskside. Region 2 Birkeland currents flow in the opposite directions at slightly lower L shells. The original meaning of the terms region 1 and region 2 as defined by *Iijima and Potemra* [1976] pertained to currents observed at ionospheric heights. In this study we consider the magnetic disturbances produced by the complete three-dimensional current systems that are the extensions of the ionospheric region 1 and 2 current systems into the magnetosphere. The terms region 1 and 2 should be understood in this sense throughout the remainder of this paper.

As noted above, the magnetosheath magnetic field "penetrates" into the magnetosphere when the magnetopause does not support the currents needed for perfect shielding. In one possible scenario the Chapman–Ferraro current is disrupted and diverted as field-aligned currents to the dayside cusp [*Coroniti and Kennel*, 1973; *Maezawa*, 1974; *Yasuhara et al.*, 1975; *Pudovkin et al.*, 1986]. The field-aligned currents flow toward the ionosphere at prenoon local times and away from the ionosphere at postnoon local times, that is, similar to the sense of region 1 Birkeland currents observed at low altitudes. However, ground observations provide no evidence for such a dayside current wedge [*Eather et al.*, 1979; *McPherron*, 1991]. Therefore some aspects of the current diversion conjecture have not yet been confirmed.

Hill and Rassbach [1975] noted that region 1 Birkeland currents depress magnetic field strengths within the dayside magnetosphere and therefore cause the dayside magnetopause to lie nearer Earth than it would in their absence. Since the region 1 Birkeland current densities increase sharply with southward IMF B_z [*Iijima and Potemra*, 1982], one would expect inward magnetopause motion to be associated with a southward IMF turning. *Maltsev and Lyatsky* [1975] presented a crude (two wire) model for the Birkeland currents and argued that the amplitude of the Birkeland currents were consistent with the observed inward magnetopause motion.

A more accurate evaluation of the magnetic disturbance produced in the outer magnetosphere by Birkeland currents is more difficult. While a reliable statistical picture was obtained for the field-aligned current distribution at low latitudes by *Iijima and Potemra* [1976, 1978], much controversy still exists as to where the current-carrying field lines map at larger distances from Earth and what their principal generation mechanism is [e.g., *Stern*, 1983; *Siscoe et al.*, 1991]. A quantitative answer to this question is largely model-dependent and reflects a basic problem concerning auroral magnetic field lines that pass through the regions of weak magnetic field strength: small changes in the magnitude of magnetospheric currents (including the Birkeland currents themselves) or small shifts in the footprints may lead to significant changes in the configuration of the expected electric current circuit.

As a compromise, we choose to obtain a rough picture of the global magnetospheric structure of the region 1 currents and crudely estimate their overall magnetic effects by mapping the field lines from the polar cap boundary using the empirical magnetic field model of *Tsyganenko* [1989]. Figure 1 shows a three-dimensional view of the family of field lines in the T89 model whose footprints lie on a shifted circle approximating the location of the region 1 oval as given by *Iijima and Potemra* [1978]. Only lines in the northern/dusk quarter hemisphere are shown, and the value of Kp was chosen to lie between 2^- and 2^+. For our purposes, the lines form the framework of a "wire" model, which carries current away from the duskside ionosphere and toward the dawnside ionosphere. The magnitude of the current in each wire, J, is a function of the magnetic local time of its footprint. Figure 2 shows this function, which is symmetric with respect to the noon–midnight meridional plane, passes through zero at noon and midnight, but reaches maximal and minimal values at ~9 and ~15 MLT, in accordance with Figure 3a of *Iijima and Potemra* [1976]. Note that we use a Birkeland current distribution that differs from that reported by Iijima and Potemra in the vicinity of midnight. Instead of our simple symmetric annular zone with a linear variation of the current density through zero across the midnight meridian, they report a system of two overlapped bands in which the downward current band lies poleward of the upward current band and the current density does not pass through zero at midnight. T. Potemra (personal communication, 1992) notes that field-aligned currents are essentially absent near midnight during geomagnetic quiet intervals and only appear with increasing geomagnetic activity. Thus the average field-aligned current pattern near midnight reported by *Iijima and Potemra* [1976] is

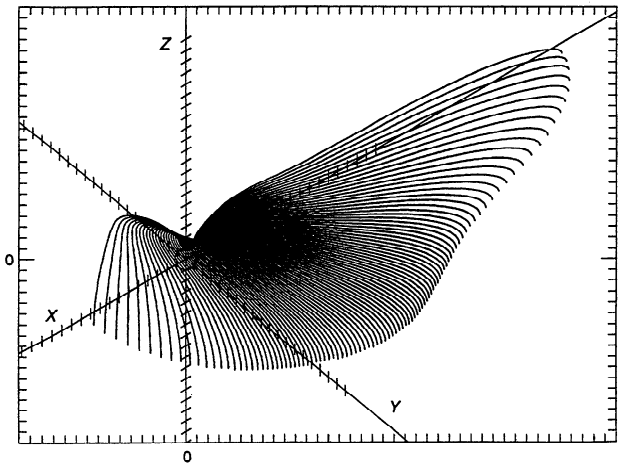

Figure 1. The family of model magnetic field lines with footprints distributed in the locations where region 1 Birkeland currents are observed. The lines correspond to the $Kp = 2^-$, 2, 2^+ version of the T89 model and form a framework for evaluating the magnetic field of Birkeland currents by means of the Biot–Savart integration. Tick marks on the axes are spaced at 1 R_E intervals.

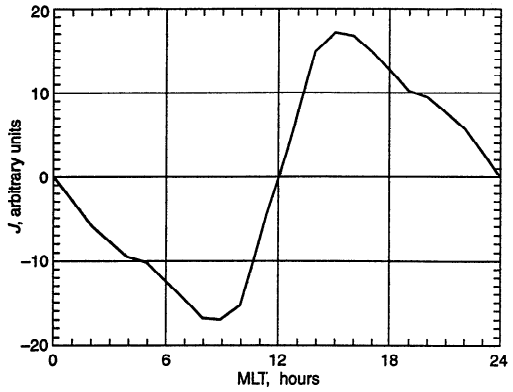

Figure 2. The local time distribution of the region 1 Birkeland current magnitude at the ionospheric level, which was used in the model to calculate the perturbation magnetic field due the region 1 Birkeland current system. The results of *Iijima and Potemra* [1976] were used to produce the plot.

not a part of the global pattern that precedes substorm onset. Instead, it represents an average over the substorm current wedges that appear abruptly in the vicinity of local midnight at substorm onset. For simplicity, we assume the current density to vary nearly linearly versus MLT within about ±4 hours from local midnight.

Having thus defined the model Birkeland current distribution, we can compute its contribution to the magnetic field at any point by performing a Biot–Savart integration. The southern hemisphere current system was assumed to carry the same amount of net current and be a mirror image of the northern one, which seems to be a reasonable assumption for the equinoxes. Figure 3 shows a plot of the B_z component of the disturbance field along the X_{gsm} axis ($B_x = B_y = 0$ by symmetry); the net magnitude of the current flowing into the northern ionosphere was set equal to 3.0 MA, a value typical of moderately disturbed geomagnetic intervals [*Bythrow and Potemra*, 1983]. As expected, the disturbance field is negative on the dayside and positive on the nightside. At the location of the subsolar point the model region 1 Birkeland current system yields $B_z \sim -10$ nT.

Note that the model current system shown in Figure 1 is not closed: we have assumed that the field-aligned currents emerge from the equatorial plane in the morning sector and flow into the equatorial plane in the evening sector. Therefore we must add a contribution from the closure currents to the field just computed for the Birkeland currents. As mentioned above, there is at present no consensus concerning the source(s) of the region 1 Birkeland currents and the configuration of the outer part of the current system. The first possibility, stemming from the concept of the disruption of the Chapman–Ferraro current (see above), is that the majority of the closure current flows on the dayside, either in the magnetosheath or within the boundary layer. In this case the westward closure current produces an additional negative contribution to the net subsolar field inside the magnetosphere, and hence the wire model shown in Figure 1 underestimates the magnitude of the negative disturbance within the dayside magnetosphere. The alternative possibility, assumed by *Siscoe et al.* [1991], is that the closure current, as in the case of the tail current system, flows in the high-latitude region adjacent to the plasma mantle. In this case the remote closure circuit would produce a small positive disturbance in the subsolar magnetosphere. Note that the closure currents must also serve, at least partially, as shielding currents that confine and compress the field due to the internal part of the electric circuit. On the basis of the above considerations, as well as on the results of shielding the tail current system (see below), we believe that the actual effect of the closure current near the subsolar point is relatively small, and hence the estimate obtained by using the wire model of Figure 1 is reasonable.

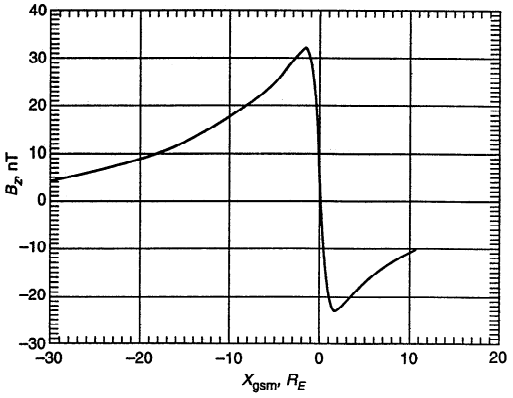

Figure 3. Variation of the B_z component of the magnetic field along the X_{gsm} axis which is produced by the model region 1 Birkeland current system, defined as shown in Figures 1 and 2.

Moreover, one must recognize that the model may somewhat overestimate the amount of Birkeland current flowing to the magnetotail and hence underestimate the current on the lines that map closer to the dayside. Indeed, a recent statistical study of the magnetotail structure by *Tsyganenko et al.* [1993] indicates that the tail field lines at $X_{gsm} = -20\,R_E$ should carry a net Birkeland current at least 3–5 times smaller than the present calculation implies. This could be explained by assuming that the Birkeland currents are diverted in the Y direction toward the dawn and dusk magnetopause due to their own shear [e.g., *Hill and Rassbach*, 1975]. However, the main contribution to the subsolar field comes from the dayside part of the region 1 current system. Hence, taking into account the shear and closure effects is unlikely to significantly change our estimate of the perturbation to the subsolar field. In short, the average contribution from the region 1 field-aligned currents at the subsolar point can be evaluated as −10 nT. During periods of strongly southward IMF B_z this value may increase by a factor of 2.

The large-scale lower-latitude region 2 system of field-aligned currents produces a magnetic field disturbance of opposite sign in the dayside magnetosphere. Because of the much smaller dimension of the region 2 circuit and the predominantly nightside location of the currents in this circuit, one expects it to make a much smaller contribution to the magnetospheric magnetic field near the subsolar magnetopause than the region 1 current system. More quantitatively, assuming for simplicity that the region 2 current loop is nearly equatorial, lies centered at $X_{gsm} \sim -5\,R_E$, has a characteristics radius of ~5 R_E, and a net current of 2 MA [*Iijima and Potemra*, 1978], one obtains a rough upper estimate for its magnetic moment as about 50% that of the Earth's dipole. That would provide for a 5-nT contribution to the magnetic field strength at the subsolar point. However, the actual distribution of the region 2 currents is even more localized [*Tsyganenko*, 1993], and hence its magnetic moment is significantly smaller. Therefore the region 2 current system cannot contribute more than a few nanoteslas to the subsolar magnetospheric magnetic field strength.

The Cross-Tail Current

A dawn-to-dusk cross-tail current in the Earth's plasma sheet is required to separate the sunward and antisunward magnetic fields within the Earth's northern and southern lobes. This magnetotail current loop is completed by a dawnward current around the magnetotail magnetopause. The net effect of the cross-tail current system is to oppose the dipole field within the dayside magnetosphere. In situ magnetotail observations require the strength of the cross-tail current in the near-Earth magnetotail to vary greatly during the course of a substorm [*Kaufmann*, 1987]. However, the results of *Unti and Atkinson* [1968] and *Schield* [1969] suggest that variations in the cross-tail current produce negligible effects upon the dayside magnetospheric magnetic field strength and therefore the location of the dayside magnetopause.

An accurate estimate of the tail contribution to the subsolar magnetic field requires a realistic model of the whole current system. Several tail current models are currently available that can reproduce basic nightside features such as the finite thickness of the equatorial current sheet, variations in current density along the tail, and the warping of the sheet in the X and Y directions in response to variations in the Earth's dipole tilt angle [*Voigt*, 1981; *Stern*, 1987, 1990; *Tsyganenko and Usmanov*, 1982; *Tsyganenko*, 1987, 1989] (the last three being referred to henceforth as the TU82, T87, and T89 models). The models of *Voigt* [1981] and *Stern* [1987] are based on a stretching deformation of the nightside magnetic field that does not imply any effect at the dayside. The TU82, T87, and T89 models are based on explicit representations for the tail current density and spacecraft data and therefore could provide a gross estimate of the tail fringe field at the dayside. However, the contribution of the closure current (which turns out to be significant) is taken into account in those models in a rather primitive way, by introducing a pair of planar current sheets parallel to the one lying in the equatorial plane. This deficiency of the tail current model was largely alleviated in the TU82, T87, and T89 models due to a flexible exponential-polynomial representation for the magnetopause magnetic field and its interplay with the tail field terms. This resulted in a good global fitting to the net observed magnetic field, but introduced some indeterminacy in attributing contributions given by individual current systems. Here we present an accurate calculation of the magnetic field produced by a realistic tail current system that includes the curvature of the current flow lines, a decrease of the current density in the antisunward direction, and a magnetopause that fully shields the tail field from the magnetosheath. As shown below, the last requirement can be used to find the unique self-shielding distribution of the closure currents.

Having this purpose in mind, we developed a purely numerical method for deriving the magnetotail magnetopause current system based upon the classic work of *Mead and Beard* [1964]. Their approach is good not only for solving the problem of the Earth's dipole shielding but also for determining the tail current. Mead and Beard divided the model magnetopause into small area elements and imposed the condition $B = 0$ outside the magnetosphere. From this an integral equation either for the shielding field or for the shielding current density follows; in the latter case it has the form [*Tsyganenko*, 1981]:

$$\mathbf{J}(\mathbf{r}) = \mathbf{n} \times \left[\frac{2}{\mu_0} \mathbf{B}_i + \frac{1}{2\pi} \int_{S-\Delta S} \frac{\mathbf{J}(\mathbf{r}') \times (\mathbf{r} - \mathbf{r}')}{|\mathbf{r} - \mathbf{r}'|^3} ds' \right] \quad (5)$$

where $\mathbf{B}_i$ is the field from an internal current system to be shielded and $\mathbf{n}$ is the inward boundary normal. The integration in (5) should be performed over the entire magnetopause surface S, except in the vicinity ΔS of the point $\mathbf{r}$. In the first approximation we ignore the integral term and obtain the first-order currents. When these are substituted into the integral, one obtains the second-order currents and so on (in practice, 5–10 iterations are enough for obtaining a self-consistent solution). Mead and Beard combined this method with a search for the self-consistent shape of the magnetopause satisfying the pressure balance condition. Here we take the boundary shape and size as being analytically prescribed [e.g., *Sibeck et al.*, 1991], which drastically simplifies the problem.

The magnetic field $\mathbf{B}_i$ in (5) corresponds to the contribution from the intramagnetospheric (equatorial) part of the tail current system, computed by Biot–Savart integration over the model current sheet between its dawn and dusk flanks. The shielding current obtained from (5) automatically turns out to be the closure current. In other words, the divergences of the currents within the current slab and shielding currents are equal and opposite at the dawn–dusk flanks and there is no current divergence for the combined current system. Figures 4 and 5 show the current flow lines in the (input) equatorial model current sheet and above the ecliptic plane in the (output) magnetopause closure current system, as iteratively computed from (5). The magnetopause shape was defined as an axially symmetric prolate ellipsoid with the dimensions given by *Sibeck et al.* [1991] for the typical range of solar wind dynamic pressures ($1.47 < p < 2.60$ nPa).

To illustrate the importance of correctly taking into account the closure currents in tail models, Figures 6 and 7 show the variation of the B_x and B_z components in the Sun–Earth direction as determined from the T87L model (dashed line) and as determined from the fully shielded tail model (solid line). For both cases we used exactly the same current density distribution along the X axis. As expected, tail lobe ($x < -10\ R_E$) distributions of B_x are nearly the same for both models. However, there is a drastic difference in the profiles of B_z in the same region. Figure 8 compares B_z profiles for two current line curvatures. The dashed line in Figure 8 is repeated from Figure 7 and

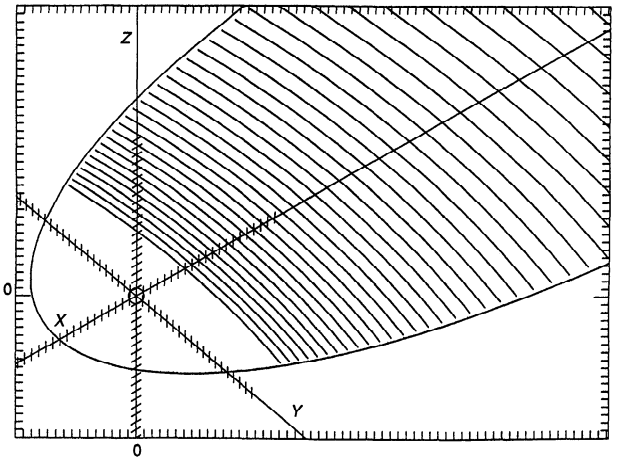

Figure 4. The model magnetotail current sheet within the ellipsoidal magnetopause that was used to evaluate the magnetic field from the fully shielded tail current system. The sheet current density is inversely proportional to the spacing between neighboring current flow lines and corresponds to that obtained in the T87 magnetic field model for $Kp = 3^-, 3, 3^+$.

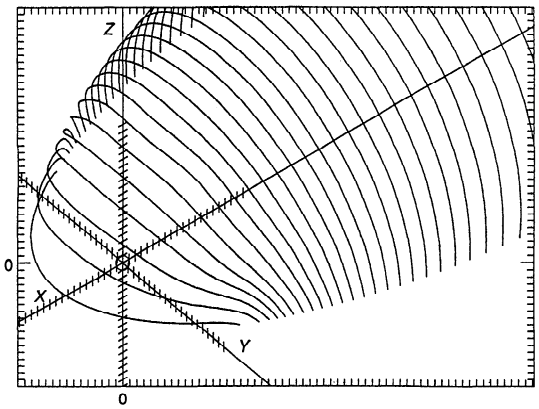

Figure 5. A family of magnetopause current flow lines that close the equatorial current sheet shown in Figure 4 and ensure complete shielding of the entire tail current system outside the model magnetosphere. The current flow lines correspond to the solution of (5), with each pair of neighboring lines bounding the same amount of net current. Only the northern half of the current system is shown, the southern half being symmetrical with respect to the equatorial plane.

corresponds to the T87L model with almost straight flow lines, whose center of curvature was placed at X_c = 100 R_E on the Earth–Sun line, whereas the solid line corresponds to the more realistic current configuration with X_c = 2.5 R_E shown in Figure 9. All our calculations indicate that the fringe field of the tail current system at the subsolar point lies between −5 and −10 nT. There is, however, strong evidence that the cross-tail current does increase dramatically in the near-Earth magnetotail during the growth phase of a substorm [e.g., *Kaufmann*, 1987], and this could result in an even larger disturbance field.

It is interesting to note that the main contribution to the subsolar magnetospheric magnetic field from the tail current system actually comes from the cross-tail segment. As for the contributions from the dayside and high-latitude magnetopause sections of the cross-tail current closure system, we note that they have opposite polarities in the subsolar region and therefore nearly cancel each other, leaving their contribution to the subsolar field less than 1 nT.

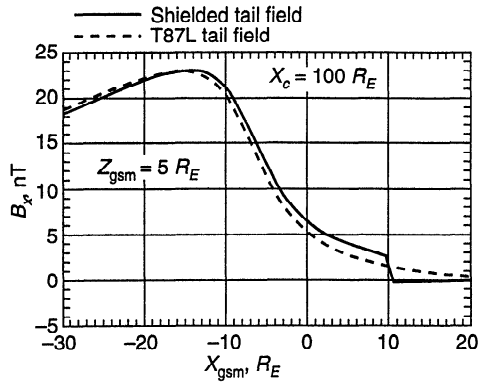

Figure 6. The variation of the B_x component of the magnetic field that is due to the fully shielded tail current system shown in Figures 4 and 5 (solid line). The variation is shown along a line parallel to the X_{gsm} axis but located at Z_{gsm} = 5 R_E. The profile obtained for the T87L model for the same current density distribution is also shown (dashed line). Note the jump of the shielded field on crossing the magnetopause at $X_{gsm} \approx 10\ R_E$.

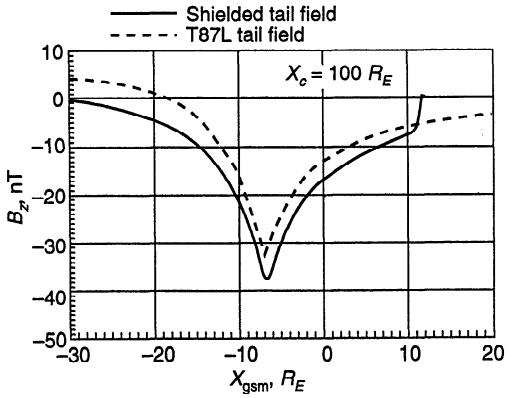

Figure 7. The variation of the B_z component along the X_{gsm} axis in the same format as that of Figure 6. The solid line corresponds to the fully shielded tail current system and the dashed line to the T87L model with the same current density.

Table 1 briefly summarizes the estimates that we have obtained for the contributions from different sources to the subsolar magnetospheric magnetic field strength.

Observations

Objectives. *Aubry et al.* [1970, 1971] presented OGO 5 observations during an inbound pass from 1500 to 2100 UT on March 27, 1968. The magnetopause observations made during this interval are central to our understanding of the solar wind–magnetosphere interaction, since this single pass has been interpreted both by the original authors and many subsequent researchers as strong evidence in favor of inward, global, dayside magnetopause motion resulting from magnetic flux erosion during a period of southward IMF. The reexamination described below confirms that there was indeed inward magnetopause motion in response to flux erosion from the dayside magnetosphere and indicates that this inward motion was very slow. We estimate its amplitude and show that it is consistent with the expected increase in cross-tail and region 1 Birkeland currents during a period of southward IMF. There is also evidence for sudden inward magnetopause motion driven by sharp increases in the solar wind dynamic pressure during the same interval.

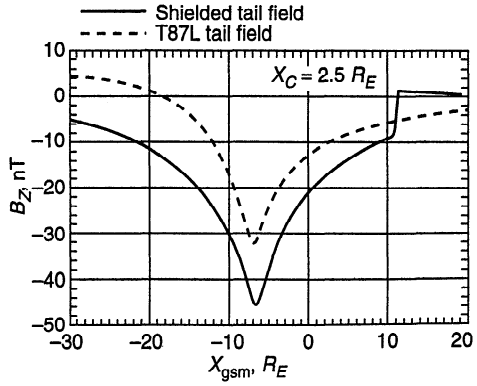

Figure 8. The variation of the B_z component along the X_{gsm} axis in the T87L model (solid line) and in the model shown in Figure 4 (X_c = 100 R_E, dashed line).

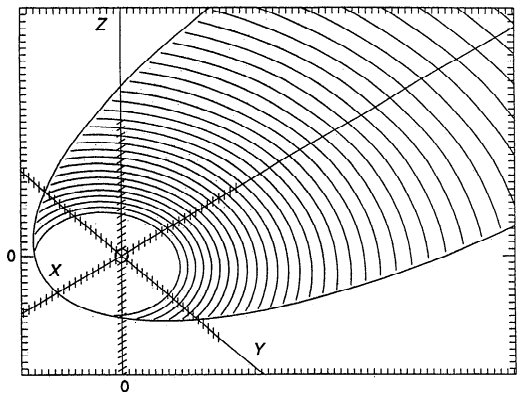

Figure 9. The model magnetotail current sheet used for calculating the plot in Figure 8. Compare with Figure 4.

Data Sets. For the purposes of this study, we will present and/or discuss Explorer 35 solar wind plasma and magnetic field observations, Explorer 33 dusk magnetosheath magnetic field observations, OGO 5 magnetosheath and magnetospheric magnetic field observations, and IMP 4 duskside magnetotail magnetic field observations during the period from 1700 to 2100 UT on March 27, 1968. The details of these observations and the original plots have already been presented by *Aubry et al.* [1970, 1971]. Figure 10 shows the locations of the relevant spacecraft during the period of interest. Explorer 35 was at lunar distance nearly directly upstream of Earth. Explorer 33 was on an inbound pass through the postnoon magnetosheath. OGO 5 was inbound on an essentially equatorial, prenoon trajectory.

Solar Wind Observations. Explorer 35 IMF and solar wind plasma observations are available from 1700 until 1815 UT, when the satellite passed behind the moon. During this interval, the satellite was in the solar wind nearly directly upstream of the Earth at lunar distance. Figure 11a shows 82 s averages of the IMF latitude in solar equatorial coordinates as measured by the Ames magnetometer on Explorer 35. Inspection of Figure 11 reveals that the latitude was northward until 1710 UT, became unsettled and less northward during the period from 1710 to 1720 UT, and then began a gradual southward turning that continued monotonically until 1740 UT. The IMF reached its most southward orientations at 1740 and 1745–1750 UT. From 1750 to 1808 UT, fluctuations in the IMF orientation were superimposed upon a gradual northward rotation. The southward turning from 1808 to 1815 UT was followed by a prolonged data gap which lasted until at least 2000 UT.

Explorer 35 solar wind plasma observations are available at 2–6 min time resolution. Prior to the interval shown, the solar wind dynamic pressure declined from a peak value of 1.2 nPa at 1637 UT to a value of 0.96 nPa at 1648 UT. The solar wind dynamic pressure remained nearly constant until 1707 UT, at which time it increased slightly to 0.98 nPa. At 1712 UT the solar wind dynamic pressure fell to 0.9 nPa. As shown in Figure 11b, the solar wind pressure rose abruptly to 1.12 nPa at 1715 UT, the steepest rise throughout the interval shown. The solar wind dynamic pressure decreased to 1.0 nPa from 1715 to 1730 UT, rose again to 1.2 nPa from 1730 to 1745 UT, fell to 1.07 nPa from 1750 to 1810 UT, reached a minimum of 0.97 nPa at 1812 UT, and rose again at 1815 UT, just before the data gap began. Consequently, the available observations indicate at least ~30% transient variations in the solar wind dynamic pressure. During this interval the solar wind velocity ranged from 461 to 497 km s^{-1}. Using the observed solar wind velocity, and the location of Explorer 35 some 60 R_E upstream of the Earth, we estimate that each feature in the solar wind required approximately 10 min to reach the subsolar bow shock at 15 R_E upstream from Earth.

Magnetosheath Observations. Explorer 33 moved inbound through the postnoon magnetosheath during the interval from 1700 to 2000 UT. Figure 11c indicates that the magnetosheath magnetic field latitude observed by Explorer 33 remained northward until 1720 UT, then began a gradual southward turning which was interrupted by fluctuations in the latter half of the hour, and ultimately culminated in a strongly southward magnetosheath magnetic field orientation at 1752 UT. The magnetosheath magnetic field orientation then rotated northward, with two northward peaks being observed at 1808 and 1816 UT. The magnetosheath magnetic field latitude continued to fluctuate until 1835 UT but was strongly southward from that time until 1900 UT. From 1900 to 1920 UT the magnetosheath magnetic field latitude rotated northward. A comparison of the magnetic field observations upstream and downstream of the bow shock indicates that features at Explorer 33 lagged those at Explorer 35 by about 10 min.

Magnetopause Observations. During the interval from 1719 to 1919 UT, OGO 5 moved inward near 0900 LT from a radial distance of 12.4 R_E to one of 9.9 R_E. Figure 12 shows OGO 5 magnetometer observations at 4.6 s time resolution during this 2-hour interval. As reported by *Aubry et al.* [1970], OGO 5 first clearly entered the magnetosphere at 1700 UT, shortly prior to the interval shown, at which time the spacecraft was located 12.81 R_E from Earth. Figure 1 of *Aubry et al.* [1970] indicates that the magnetospheric magnetic field strength just inside this magnetopause crossing was 30 nT. During the following 29 min, OGO 5 moved inward through the magnetosphere, where it observed occasional transient variations superimposed upon a gradual increase in the magnetic field strength to a value of 40

Table 1. Estimated Contributions to the Subsolar Magnetospheric Magnetic Field Strength From Various Current Systems

Dipole+CF,* nT	Ring Current, nT	Tail Current System, nT		Birkeland Currents, nT	
		Cross-Tail	Closure	Region 1	Region 2
$2f \times 23$	8 to 10	−5 to −10	~1	−10 to −20	<5
Total		−5 to −10		−10 to −20	

*We assume that the subsolar magnetopause lies 11 R_E from Earth and consider the contribution for the Earth's dipole and the portion of the Chapman–Ferraro current which shields the Earth's dipole. The factor f varies but generally lies near 1.22.

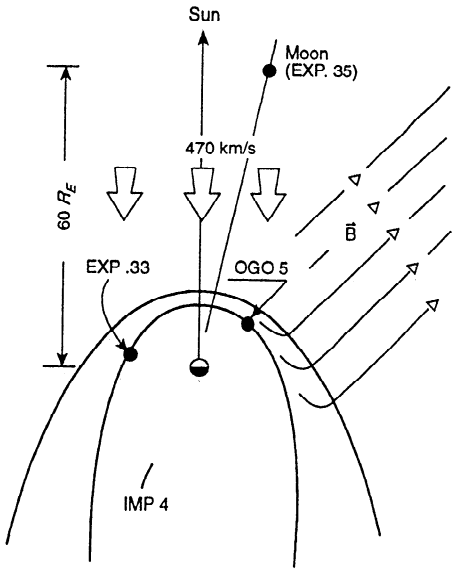

Figure 10. The locations of Explorer 35 (solar wind), Explorer 33 (magnetosheath), OGO 5 (dayside magnetopause), and IMP 4 (magnetotail) in the GSM equatorial plane on March 27, 1968 (adapted from *Aubry et al.* [1970]).

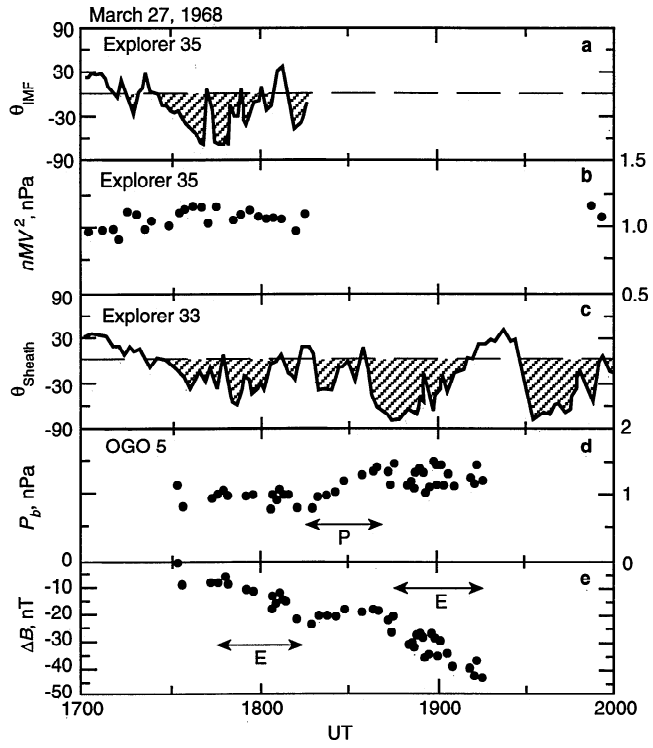

Figure 11. (a) The IMF latitude in the solar equatorial reference system as observed by Explorer 35; (b) the solar wind dynamic pressure observed by Explorer 35; (c) the magnetosheath magnetic field latitude as measured by Explorer 33; (d) the magnetic field pressure just inside each magnetopause crossing observed by OGO 5; and (e) the depression in the dayside magnetospheric magnetic field strength required in order for this magnetic field strength to be observed at the location of OGO 5. Two bars marked E indicate intervals in which OGO 5 observations were used to infer flux erosion. The bar marked P indicates an interval in which OGO 5 observations were used to infer an increase in the solar wind dynamic pressure.

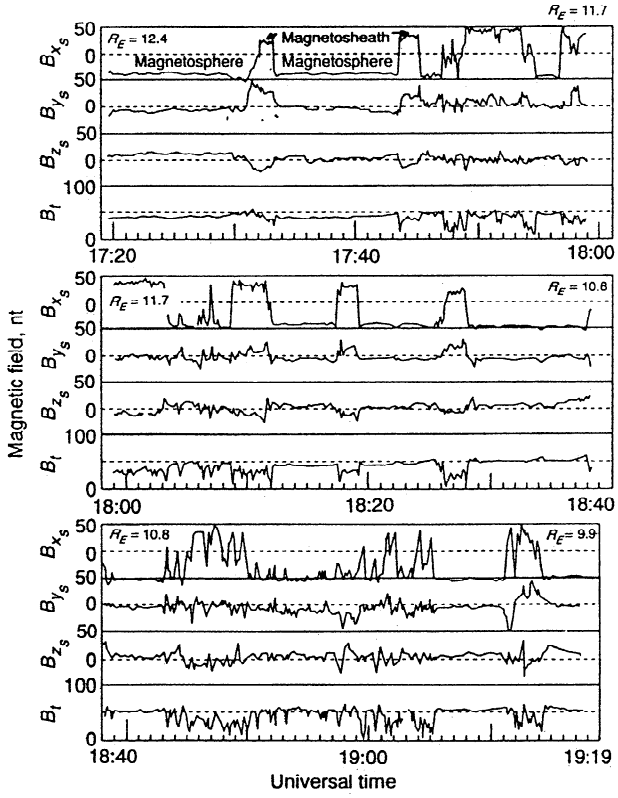

Figure 12. OGO 5 magnetic field observations from 1719 to 1919 UT on March 27, 1968 (adapted from *Aubry et al.* [1970]). The observations are shown in the reference system of the satellite, where the X direction lies within 10° of the negative Z_{gsm} axis.

nT. As shown in Figure 12, the magnetospheric magnetic field strength increased sharply from 40 to 60 nT from 1729 to 1731 UT, at which time the spacecraft exited the magnetosphere and entered the magnetosheath at a radial distance from Earth of 12.4 R_E. The subsequent sequence of over 40 partial or complete magnetopause crossings was terminated by a final entry into the magnetosphere at 1914 UT.

Aubry et al. [1970, 1971] identified three separate timescales associated with the magnetopause motion. The first was a 2 R_E inward motion of the mean magnetopause position in a period of 2 hours following the 1710–1715 UT reversal of the IMF, which they attributed to magnetic flux erosion from the dayside magnetosphere. The second was a long-period (T = 3.5 to 6 min) magnetopause motion, which they attributed to the Kelvin–Helmholtz instability at the magnetopause. The third was a short-period (10–60 s) motion, for which they provided no explanation. In this paper we will be concerned primarily with the long-period motion associated with flux erosion.

Inward Motion of the Mean Magnetopause Position Caused by an Enhanced Solar Wind Dynamic Pressure. We attribute the OGO 5 entry into the magnetosphere at 1700 UT to outward motion of the magnetopause driven by a decrease in the solar wind dynamic pressure, the OGO 5 exit from the magnetosphere at 1731 UT to a sharp increase in the solar wind dynamic pressure, argue that the magnetopause moved gradually inward between 1731 and 1805 UT in response to a southward interplanetary and magnetosheath magnetic field orientation, and maintain that the magnetopause moved inward from 1820 to 1840 UT in response to an unobserved increase in the solar wind

dynamic pressure. We concur with *Aubry et al.* [1970] that the magnetopause again moved inward after 1840 UT in response to a second interval of southward IMF. In this section we discuss the evidence for magnetopause motion in response to changes in the solar wind dynamic pressure.

We have already commented upon Explorer 35 observations of a sharp decrease in the solar wind dynamic pressure from 1637 to 1648 UT and a sharp increase at 1715 UT. We noted that at least 10 min were required for features at Explorer 35 to reach Explorer 33. A longer time would have been required for features to reach the subsolar magnetopause and for the magnetosphere to respond. Thus the 1637–1648 UT decrease in the solar wind dynamic pressure should have led to outward magnetopause motion sometime during or after the interval from 1647 to 1658 UT, consistent with the OGO 5 entry into the magnetosphere at 1700 UT. And the transient increase in the solar wind dynamic pressure from 1715 to 1718 UT should have produced sharp inward magnetopause motion sometime during or immediately after the interval from 1725 to 1728 UT, consistent with a brief exit by OGO 5 into the magnetosheath at 1731 UT.

As discussed earlier, outer magnetospheric magnetic field observations themselves provide important information concerning variations in the solar wind dynamic pressure and the region 1 Birkeland currents. For example, Figure 12 shows that there was indeed an enhancement in the magnetospheric magnetic field strength from 40 to 60 nT during the interval from 1729 to 1731 UT, indicative of a sudden inward magnetopause compression caused by an increase in the solar wind dynamic pressure just prior to the OGO 5 magnetopause crossing at 1731 UT. This inward magnetopause motion was not caused by the arrival of the southward IMF turning at the magnetopause, since the onset of merging launches a fast rarefaction wave into the magnetosphere which decreases the magnetospheric magnetic pressure and allows magnetopause pressure balance to be reestablished at a location nearer Earth.

Figure 11d shows the magnetospheric magnetic pressures ($= B^2/2\mu_0$) observed just inside each subsequent OGO 5 magnetopause crossing as a function of time. As shown in Figure 11d, the magnetic pressure just inside the magnetopause remained within the range from 0.8 to 1.1 nPa prior to 1830 UT but subsequently increased to lie within the range from 1.1 to 1.5 nPa from 1830 to 1915 UT. By (1), this approximately 50% increase in magnetospheric magnetic pressures indicates a similar increase in the unreported solar wind dynamic pressure during the period from 1820 to 1840 UT. *Russell et al.* [1974] suggested that the increase in magnetospheric field strengths and pressures resulted from the gradual motion of OGO 5 toward the subsolar magnetopause and the interception of a greater solar wind dynamic pressure due to the gradual flaring of the magnetopause in response to the southward IMF. Note, however, that the observed increase does not transpire gradually over the entire 2-hour interval nor over the two periods in which the magnetosheath magnetic field pointed strongly southward, but rather from 1820 to 1840 UT, a period in which the magnetosheath magnetic field did not point strongly southward.

Having inferred that there was a sudden increase in solar wind dynamic pressure applied to the magnetosphere during the period from 1820 to 1840 UT, the next question must be to determine whether or not it suffices to explain the observed inward magnetopause motion. Like *Aubry et al.* [1970] and *Sibeck et al.* [1991], for simplicity we suppose that the shape of the magnetosphere remains nearly self-similar during inward contractions in response to variations in solar wind dynamic pressure. Then the distance to the magnetopause depends approximately on the sixth root of the solar wind dynamic pressure. A 50% increase in the solar wind dynamic pressure results in a 7% decrease in the magnetopause position. At 1800 UT, OGO 5 was 11.7 R_E from Earth and in the midst of a series of magnetopause crossings during which the satellite spent approximately equal times inside and outside the magnetosphere. The inferred 50% increase in solar wind dynamic pressure from 1820 to 1840 UT should have moved the magnetopause inward to about 10.9 R_E. Since the magnetopause was subsequently observed 10 R_E from Earth at 1900 UT, the inferred increase in solar wind dynamic pressure does not suffice to explain all of the observed magnetopause motion.

Inward Motion of the Mean Position of the Magnetopause in Response to Magnetic Merging and an Increase in the Magnetospheric Currents. We have seen that there is evidence for sudden inward motion of the mean magnetopause position in response to both observed and inferred increases in the solar wind dynamic pressure on March 27, 1968. However, the amplitude of the observed inward magnetopause motion exceeds that associated with the increases in solar wind dynamic pressure. It is therefore necessary to find another mechanism responsible for gradual inward magnetopause motion over time periods of 30 min to 2 hours. The most likely candidate for such motion is flux erosion from the dayside magnetosphere, as originally proposed by *Aubry et al.* [1970].

To identify intervals of magnetic flux erosion from the dayside magnetosphere, we must identify intervals of southward interplanetary and magnetosheath magnetic fields. As discussed above, Explorer 35 observations indicate that the IMF became less northward and fluctuated from 1710 to 1720 UT, but was southward from 1720 to 1755 UT, corresponding to a generally southward magnetosheath magnetic field observed by Explorer 33 from 1730 to 1805 UT. IMF observations ended shortly thereafter, but magnetosheath magnetic field observations indicated northward and southward fluctations during the period from 1805 to 1840 UT. The magnetosheath magnetic field turned sharply southward at 1840 UT and remained in this orientation for the next 30 min. On the basis of these observations we would expect significant inward magnetopause motion to have resulted from flux erosion during the periods from 1730 to 1805 and 1840 to 1910 UT.

Again, it is the OGO 5 observations themselves that provide the strongest evidence for this inward erosion in the mean position of the magnetopause. Equation (2) shows that the magnetic field just inside the magnetopause has many possible sources, but we have argued above that contributions from the dipole, region 1 Birkeland currents, and the cross-tail current are most important on the timescales of interest here. As above, we adopt the assumption that B_{cf} and B_{rc} are proportional to B_d and solve (2) for the contributions to the subsolar magnetospheric magnetic field strength from the region 1 Birkeland and cross-tail currents as a function of the position of OGO 5:

$$B_b + B_t = B - B(t_0)R_0^3/R^3 \qquad (6)$$

We assume that the magnetopause was in pressure balance without any contribution from the Birkeland and cross-tail currents at t_0 = 1731 UT and R_s = 12.7 R_E. The latter assumption is justified by the northward interplanetary and magnetosheath magnetic fields prior to this time. Figure 11e shows the variation of $B_b(t) + B_t(t)$ as deduced from (6). If variations in the solar

wind dynamic pressure were the sole cause of the magnetopause motion on this day, the magnetospheric magnetic field strength observed just inside each magnetopause crossing (B) would vary as $1/R^3$, that is, the right side of (6) would vanish. Because the observed magnetic field strength just inside each magnetopause does not rise as rapidly as $1/R^3$ as the spacecraft moves inward, the value of $B_b + B_t$ becomes increasingly negative with time. The depression of the outer magnetospheric magnetic field caused by the Birkeland and cross-tail currents is required to increase from 0 to −50 nT over the entire interval. The steepest increases occur from 1745 to 1815 UT and from 1845 to 1915 UT. Comparison with the magnetosheath magnetic field observations shown in Figure 11b indicates that these two intervals are those during which the magnetosheath magnetic field orientation turned and remained southward. By contrast, no enhancement in the depression of dayside magnetospheric magnetic field strengths is required from 1815 to 1845 UT, during which the dayside magnetosheath magnetic field orientation turned northward and fluctuated greatly.

The inferred steady increases in region 1 Birkeland and cross-tail current strengths and the concomitant depressions of the dayside magnetospheric magnetic field strength imply that the location of the dayside magnetopause moved steadily inward during the 1745–1815 and 1845–1910 UT intervals. While there is no evidence contradicting such inward dayside magnetopause motion from 1845 to 1910 UT, *Aubry et al.* [1970] noted that OGO 5 spent most of the early part of the interval from 1730 to 1830 UT in the magnetosheath, but most of the later part in the magnetosphere. They concluded that this indicated a nearly stationary mean position of the magnetopause near 11.6 R_E. The observations can be reconciled if the magnetopause is allowed to move steadily inward during the period from 1745 to 1815 UT, but at a slower rate than OGO 5. We can estimate the inward rate of magnetopause motion during the 1745–1815 UT interval. As discussed above, the observed and inferred increases in solar wind dynamic pressure can account for an approximately 0.8 R_E inward motion of the magnetopause, but the full range of observed magnetopause locations from 1800 to 1900 UT was 1.7 R_E. If we attribute the remaining 0.9 R_E variation in magnetopause position to the increases in Birkeland current, then 40% should be assigned to the interval from 1745 to 1815 UT during which the inferred depression in the magnetospheric magnetic field strength increased from 0 to −20 nT and about 60% should be assigned to the interval from 1845 to 1910 UT during which the inferred depression increased from −20 to −50 nT. The required rate of inward motion during the first interval is then 0.36 R_E in 25 min or 1.5 km s^{-1}. During the same interval, OGO 5 moved inward at a velocity of 2.5 km s^{-1}. If we make the assumption that the amplitude of the quasi-periodic magnetopause motion remained nearly constant, then the relatively faster inward motion of the satellite during this period implies that the proportion of time that OGO 5 spends in the magnetosheath must diminish, as reported by *Aubry et al.* [1970].

We have used solar wind and dayside magnetopause crossings to infer steady inward magnetopause motion and dayside magnetospheric magnetic flux erosion during the periods from 1745 to 1815 and 1845 to 1910 UT. *Aubry et al.* [1970] presented IMP 4 magnetotail observations that showed enhanced magnetic field strengths and depressed values of B_z from 1730 to 1805 UT, a decrease in the magnetotail magnetic field strength and an increase in the B_z after 1805 UT, an increase in magnetotail magnetic field strength and a decrease in B_z beginning at 1850 UT (although they called out a time of 1840 UT) and continuing until 1915 UT, and a decrease in tail field strengths and increase in B_z beginning at 1937 UT. The enhanced magnetotail field strengths from 1730 to 1805 UT may indicate compression of the magnetotail by the increase in solar wind dynamic pressure following 1730 UT. The fact that the magnetotail magnetic field strength remained nearly constant from 1730 to 1805 UT indicates that the inferred decrease in dayside magnetospheric magnetic field strengths during the interval from 1745 to 1815 UT did not correspond to an increase in cross-tail currents. The reason for the decrease in magnetotail magnetic field strengths from 1805 to 1850 UT remains unclear. Like *Aubry et al.* [1970] we attribute the increase in magnetotail magnetic field strengths after 1850 UT to the deposition of flux eroded from the dayside magnetosphere into the magnetotail. Of course, the increasing magnetotail magnetic field strengths require an increase in the cross-tail current, and this in turn must correspond to a decrease in the dayside magnetospheric magnetic field strength.

Conclusions

If the magnetopause lies at rest along the locus of points where magnetosheath and magnetospheric pressures balance, inward magnetopause motion during periods of constant solar wind dynamic pressure implies a decrease in the outer magnetospheric magnetic field strength and pressure. Such decreases should be attributed to variations in magnetospheric currents rather than to a penetrating IMF. In this paper we evaluated the contributions of the ring, Birkeland, and cross-tail currents to the magnetic field strength in the outer dayside magnetosphere. Our estimates indicate that variations in the ring current generally do not contribute significantly to the outer dayside magnetospheric magnetic field strength nor drive substantial magnetopause motion over periods of 1–2 hours.

We demonstrated that variations in both the region 1 Birkeland current system and the tail currents can produce substantial (10–20 nT each) perturbations in the magnetic field strength just inside the dayside magnetopause. Perturbations of this magnitude suffice to account for the observed magnetopause motion during periods of southward IMF B_z [*Sibeck et al.*, 1991]. Initial reports by *Mal'kov and Sergeyev* [1991] and *Sibeck* [1994] indicate that pronounced tailward stretching of nightside magnetospheric magnetic field lines accompanies decreases in the dayside magnetospheric magnetic field strength during periods of prolonged southward IMF. The depressions in the dayside magnetospheric magnetic field strength might result from the disruption of Chapman–Ferraro currents and their diversion to the ionosphere in the form of dayside region 1 Birkeland currents. The lack of any evidence for a very large (several tens of nanoteslas) positive B_z perturbation in the near-Earth magnetotail requires the majority of any such Birkeland current increase to be localized in the dayside magnetosphere. By contrast, enhancements in tail current system must stretch the magnetotail field lines and produce significant depressions in both the dayside and near-Earth nightside magnetosphere. Systematic study of inner magnetospheric magnetic field strength variations during substorms should permit the effects of the two current systems to be distinguished.

We reexamined a previously reported sequence of OGO 5 magnetopause crossings that has been interpreted as strong evidence in favor of magnetic flux erosion from the dayside magnetosphere and confirmed this interpetation. We associated

two magnetopause crossings with sharp changes in the solar wind dynamic pressure and used the OGO 5 themselves to infer a further increase in the solar wind dynamic pressure from 1820 to 1840 UT. The latter increase in the solar wind dynamic pressure should have produced an approximately $0.8\,R_E$ inward magnetopause displacement. Since the magnetopause moved inward a total of $1.7\,R_E$ from 1800 to 1900 UT, we attributed the remaining $0.9\,R_E$ displacement to two intervals of magnetic flux erosion. We demonstrated that these intervals of flux erosion corresponded to two periods of southward interplanetary and magnetosheath magnetic field orientation, from 1745 to 1815 and 1845 to 1910 UT. The second period of inward magnetopause erosion corresponded to an interval of increasing tail field strength which was terminated by a substorm onset.

Acknowledgments. This work was performed while one of us (N.A.T.) held a National Research Council–GSFC Research Associateship. We thank V. Sergeev for comments concerning Russian sector ground magnetograms and M. Peredo for assistance with model calculations. We thank the NSSDC for supplying Explorer 33 and 35 observations. Work at JHU/APL was supported by NASA under Task 1 of Space and Naval Warfare Systems Command contract N00039-91-C-0001 to the Navy.

The Editor thanks T. J. Rosenberg, T. Pulkkinen, and three other referees for their assistance in evaluating this paper.

References

Aubry, M. P., C. T. Russell, and M. G. Kivelson, Inward motion of the magnetopause before a substorm, *J. Geophys. Res.*, *75*, 7018–7031, 1970.

Aubry, M. P., M. G. Kivelson, and C. T. Russell, Motion and structure of the magnetopause, *J. Geophys. Res.*, *76*, 1673–1696, 1971.

Bythrow, P. F., and T. A. Potemra, The relationship of total Birkeland currents to the merging electric field, *Geophys. Res. Lett.*, *10*, 573–576, 1983.

Cahill, L. J., Jr., and V. L. Patel, The boundary of the geomagnetic field, August to November, 1961, *Planet. Space Sci.*, *15*, 997–1033, 1967.

Chapman, S., and J. Bartels, *Geomagnetism*, p. 272, Clarendon, Oxford, 1940.

Chapman, S., and V. C. A. Ferraro, A new theory of magnetic storms, 1, The initial phase (continued), *J. Geophys. Res.*, *36*, 171–186, 1931.

Coroniti, F. V., and C. F. Kennel, Can the ionosphere regulate magnetospheric convection?, *J. Geophys. Res.*, *78*, 2837–2851, 1973.

Cowley, S. W. H., and W. J. Hughes, Observation of an IMF sector effect in the Y magnetic field component at geostationary orbit, *Planet. Space Sci.*, *31*, 73–90, 1983.

Eather, R. H., S. B. Mende, and E. J. Weber, Dayside aurora and relevance to substorm current systems and dayside merging, *J. Geophys. Res.*, *84*, 3339–3359, 1979.

Fairfield, D. H., Average and unusual locations of the Earth's magnetopause and bow shock, *J. Geophys. Res.*, *76*, 6700–6716, 1971.

Freeman, J. W., Jr., The morphology of the electron distribution in the outer radiation zone and near the magnetospheric boundary as observed by Explorer 12, *J. Geophys. Res.*, *69*, 1691–1723, 1964.

Hill, T. W., and M. E. Rassbach, Interplanetary magnetic field direction and the configuration of the dayside magnetosphere, *J. Geophys. Res.*, *80*, 1–6, 1975.

Holzer, R. E., and J. A. Slavin, Magnetic flux transfer associated with expansions and contractions of the dayside magnetosphere, *J. Geophys. Res.*, *83*, 3831–3839, 1978.

Iijima, T., and T. A. Potemra, The amplitude distribution of field-aligned currents at northern high latitudes observed by Triad, *J. Geophys. Res.*, *81*, 2165–2174, 1976.

Iijima, T., and T. A. Potemra, Large-scale characteristics of field-aligned currents associated with substorms, *J. Geophys. Res.*, *83*, 599–615, 1978.

Iijima, T., and T. A. Potemra, The relationship between interplanetary quantities and Birkeland current densities, *Geophys. Res. Lett.*, *9*, 442–445, 1982.

Kaufmann, R. L., Substorm currents: Growth phase and onset, *J. Geophys. Res.*, *92*, 7471–7486, 1987.

Kovner, M. S., Dependence of the position of the magnetopause on the orientation of the interplanetary magnetic field, *Geomagn. Aeron.*, Engl. Transl., *12*, 823–825, 1972.

Kovner, M. S., and Ya. I. Feldstein, On solar wind interaction with the Earth's magnetosphere, *Planet. Space Sci.*, *21*, 1191–1211, 1973.

Maezawa, K., Dependence of the magnetopause position on the southward interplanetary magnetic field, *Planet. Space Sci.*, *22*, 1443–1453, 1974.

Maezawa, K., Magnetotail boundary motion associated with geomagnetic substorms, *J. Geophys. Res.*, *80*, 3543–3548, 1975.

Mal'kov, M. V., and V. A. Sergeyev, Characteristics anomalies of the magnetospheric configuration under stable convection activity, *Geomagn. Aeron.*, *31*, 578–580, 1991.

Maltsev, Yu. P., and W. B. Lyatsky, Field-aligned currents and erosion of the dayside magnetopause, *Planet. Space Sci.*, *23*, 1257–1260, 1975.

McPherron, R. L., Physical processes producing magnetospheric substorms and magnetic storms, in *Geomagnetism*, vol. 4, edited by J. A. Jacobs, pp. 687–689, Academic, San Diego, Calif., 1991.

Mead, G. D., Deformation of the geomagnetic field by the solar wind, *J. Geophys. Res.*, *69*, 1181–1195, 1964.

Mead, G. D., and D. B. Beard, Shape of the geomagnetic field and solar wind boundary, *J. Geophys. Res.*, *69*, 1169–1179, 1964.

Paschmann, G., I. Papamastorakis, W. Baumjohann, N. Sckopke, C. W. Carlson, B. U. Ö. Sonnerup, and H. Lühr, The magnetopause for large magnetic shear: AMPTE/IRM observations, *J. Geophys. Res.*, *91*, 11,099–11,115, 1986.

Petrinec, S. M., and C. T. Russell, External and internal influences on the size of the dayside terrestrial magnetosphere, *Geophys. Res. Lett.*, *20*, 339–342, 1993.

Petrinec, S. M., P. Song, and C. T. Russell, Solar cycle variations in the size and shape of the magnetopause, *J. Geophys. Res.*, *96*, 7893–7896, 1991.

Potemra, T. A. (Ed.), *Magnetospheric Physics*, *Geophys. Monogr. Ser.*, vol. 28, AGU, Washington, D. C., 1984.

Pudovkin, M. I., N. A. Tsyganenko, and A. V. Usmanov, The influence of longitudinal currents on the magnetopause on the structure and position of polar cusps, *Geomagn. Aeron.*, Engl. Transl., *26*, 801–805, 1986.

Roelof, E. C., and D. G. Sibeck, The magnetopause shape as a bivariate function of IMF B_z and solar wind dynamic pressure, *J. Geophys. Res.*, *98*, 21,421–21,450, 1993.

Russell, C. T., M. Neugebauer, and M. G. Kivelson, Ogo-5 observations of the magnetopause, in *Correlated Interplanetary and Magnetospheric Observations*, edited by D. E. Page, pp. 139–157, D. Reidel, Norwell, Mass., 1974.

Schield, M. A., Pressure balance between solar wind and magnetosphere, *J. Geophys. Res.*, *74*, 1275–1286, 1969.

Sibeck, D. G., A model for the transient magnetospheric response to sudden solar wind dynamic pressure variations, *J. Geophys. Res.*, *95*, 3755–3771, 1990.

Sibeck, D. G., Signatures of flux erosion from the dayside magnetosphere, *J. Geophys. Res.*, in press, 1994.

Sibeck, D. G., R. E. Lopez, and E. C. Roelof, Solar wind control of the magnetopause shape, location, and motion, *J. Geophys. Res.*, *96*, 5489–5495, 1991.

Siscoe, G. L., W. Lotko, and B. U. Ö. Sonnerup, A high-latitude, low-latitude boundary layer model of the convection current system, *J. Geophys. Res.*, *96*, 3487–3495, 1991.

Spreiter, J. R., A. L. Summers, and A. Y. Alksne, Hydromagnetic flow around the magnetosphere, *Planet. Space Sci.*, *14*, 223–253, 1966.

Stern, D. P., The origins of Birkeland currents, *Rev. Geophys. Space Phys.*, *21*, 125–138, 1983.

Stern, D. P., Parabolic harmonics in magnetospheric modeling: The main dipole and the ring current, *J. Geophys. Res.*, *90*, 10,851–10,863, 1985.

Stern, D. P., Tail modeling in a stretched magnetosphere 1. Methods and transformations, *J. Geophys. Res.*, *92*, 4437–4448, 1987.

Stern, D. P., A model of the magnetospheric tail with current-free lobes, *Planet. Space Sci.*, *38*, 255–261, 1990.

Tsyganenko, N. A., Numerical models of quiet and disturbed geomagnetic fields in the cislunar part of the magnetosphere, *Ann. Geophys.*, *37*, 381–391, 1981.

Tsyganenko, N. A., Global quantitative models of the geomagnetic field in the cislunar magnetosphere for different disturbance levels, *Planet. Space Sci.*, *35*, 1347–1358, 1987.

Tsyganenko, N. A., A magnetospheric magnetic field model with a warped tail current sheet, *Planet. Space Sci.*, *37*, 5–20, 1989.

Tsyganenko, N. A., A global analytical representation of the magnetic field produced by the Region 2 Birkeland current and the partial ring current, *J. Geophys. Res.*, *98*, 5677–5690, 1993.

Tsyganenko, N. A., and A. V. Usmanov, Determination of the magnetospheric current system parameters and development of experimental geomagnetic field models based on data from IMP and HEOS satellites, *Planet. Space Sci.*, *30*, 985–998, 1982.

Tsyganenko, N. A., D. P. Stern, and Z. Kaymaz, Birkeland currents in the plasma sheet, *J. Geophys. Res.*, *98*, 19,455–19,464, 1993.

Unti, T., and G. Atkinson, Two-dimensional Chapman–Ferraro problem with neutral sheet, 1, The boundary, *J. Geophys. Res.*, *73*, 7319–7327, 1968.

Voigt, G.-H., Influence of the interplanetary magnetic field on the position of the dayside magnetopause, in *Magnetospheric Boundary Layers*, edited by B. Battrick, *Eur. Space Agency Spec. Publ.*, *148*, pp. 315–321, 1979.

Voigt, G.-H., A mathematical magnetospheric field model with independent physical parameters, *Planet. Space Sci.*, *29*, 1–20, 1981.

Voigt, G.-H., Magnetospheric equilibrium configurations and slow adiabatic convection, in *Solar Wind-Magnetosphere Coupling*, edited by Y. Kamide and J. A. Slavin, pp. 233–273, Terra, Tokyo, 1986.

Yasuhara, F., Y. Kamide, and S.-I. Akasofu, A modelling of the magnetospheric substorm, *Planet. Space Sci.*, *23*, 575–578, 1975.

D. G. Sibeck, Applied Physics Laboratory, Johns Hopkins University, Laurel, MD 20723. (e-mail: SPAN aplsp::sibeck)

N. A. Tsyganenko, NASA Goddard Space Flight Center, Greenbelt, Maryland 20771. (e-mail: Internet vasold@space.phys.lgu.spb.su)

(Received September 27, 1993; revised March 10, 1994; accepted March 14, 1994.)